

Unexpected Metal-Induced Isomerisms and Phosphoryl Migrations in Pt(II) and Pd(II) Complexes of the Functional Phosphine 2-(Bis(diphenylphosphino)methyl)-oxazoline[†]

Shuanming Zhang, Roberto Pattacini, and Pierre Braunstein*

Laboratoire de Chimie de Coordination, Institut de Chimie (UMR 7177 CNRS), Université de Strasbourg, 4 rue Blaise Pascal, F - 67081 Strasbourg, France

Supporting Information

ABSTRACT: The reaction of the functional diphosphine **1** [**1** = 2-(bis(diphenylphosphino)methyl)-oxazoline] with [PtCl₂(NPh)₂] or [PdCl₂(NPh)₂], in the presence of excess

NEt₃, affords [Pt{(Ph₂P)₂C···C(···NCH₂CH₂O)}₂] ([Pt-

(**1**_{-H}-P,P)₂], **3a**) and [Pd{(Ph₂P)₂C···C(···NCH₂CH₂O)}₂] ([Pd(**1**_{-H}-P,P)₂], **3b**), respectively, in which **1**_{-H} is (oxazoline-2-yl)bis(diphenylphosphino)methanide. The reaction of **3b** with 2 equiv of [AuCl(tht)] (tht = tetrahydrothiophene) afforded [Pd-

(**1**_{-H}-P,N)₂(AuCl)₂] (**4**), as a result of the opening of the four-membered metal chelate since ligand **1**_{-H}, which was P,P-chelating in **3b**, behaves as a P,N-chelate toward the Pd(II) center in **4** and coordinates to Au(I) through the other P donor. In the absence of a base, the reaction of ligand **1** with [PtCl₂(NPh)₂] in MeCN or CH₂Cl₂ afforded the isomers [Pt{(Ph₂P)₂C=

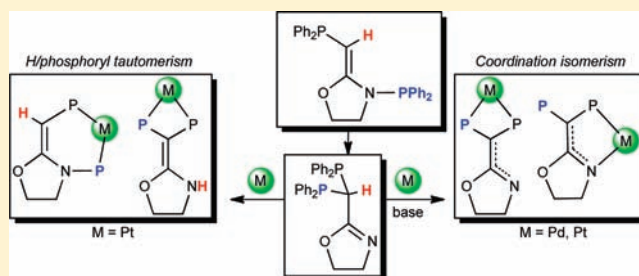
C(OCH₂CH₂NH)}₂]Cl₂ ([Pt(**1'**-P,P)₂]Cl₂ (**5**), **1'** = 2-(bis(diphenylphosphino)methylene)-oxazolidine) and [Pt{(Ph₂P)₂C=

C(OCH₂CH₂NH)}{Ph₂PCH=C(OCH₂CH₂N(PPh₂))}]Cl₂ ([Pt(**1'**-P,P)(**2'**-P,P)]Cl₂ (**6**), **2'** = (*E*)-3-(diphenylphosphino)-2-

((diphenylphosphino)methylene)oxazolidine]. The P,P-chelating ligands in **5** result from a tautomeric shift of the C–H proton of **1** to the nitrogen atom, whereas the formation of one of the P,P-chelates in **6** involves a carbon to nitrogen phosphoryl migration. The reaction of **5** and **6** with a base occurred by deprotonation at the nitrogen to afford **3a** and [Pt{(Ph₂P)₂C···

C(···NCH₂CH₂O)}{Ph₂PCH=COCH₂CH₂N(PPh₂)}]Cl ([Pt(**1**_{-H}-P,P)(**2'**-P,P)]Cl (**7**), respectively. In CH₂Cl₂, an isomer

of **3a**, [Pt{(Ph₂P)₂C···C(···NCH₂CH₂O)}{Ph₂PC(PPh₂)=COCH₂CH₂N}] ([Pt(**1**_{-H}-P,P)(**1**_{-H}-P,N)] (**8**)), was obtained as a side product which contains ligand **1**_{-H} in two different coordination modes. Complexes **3b**·4CH₂Cl₂, **4**·CHCl₃, **6**·2.5CH₂Cl₂, and **8**·CH₂Cl₂ have been structurally characterized by X-ray diffraction.



INTRODUCTION

The rich chemistry of bis(diphenylphosphino)methane (dppm)¹ can be further extended by functionalization of the central carbon atom (Scheme 1) and the introduction of donor groups (e.g., N, O, S), providing access to additional coordination modes, different from the usual P,P-chelating or -bridging modes.

For example, 2{bis(diphenylphosphino)methyl}pyridine (Scheme 2) gives rise to a variety of dinuclear complexes, some of which show a μ - $\kappa^1(P)$: $\kappa^2(P,N)$ coordination mode (type A or B, Scheme 2).² This ligand can also coordinate in a tripodal η^3 -N, P,P fashion to Cr,³ Mo, W,⁴ Re,⁵ and Ru, Rh,⁶ Ir³ (type C, Scheme 2) or in a P,N- (on Fe, Cd, Re)³ (type D, Scheme 2) or

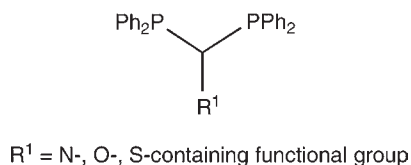
P,P-chelating mode (on Fe)³ (type E, Scheme 2). Bonding mode B was also observed in the case of 2-{bis(diisopropylphosphino)methyl}-1-methylimidazole coordinated to Cu(I) and Ag(I) centers, the resulting dinuclear complexes displaying a significant metal–metal interaction.⁷

However, the coordinated ligand 2-{bis(diphenylphosphino)methyl}pyridine has rarely been described in its deprotonated form.³ Furthermore, the aromaticity of the pyridine ring and the low basicity of its N function disfavor migration of the PCHP proton or of one of the phosphoryl groups to this nitrogen, thus

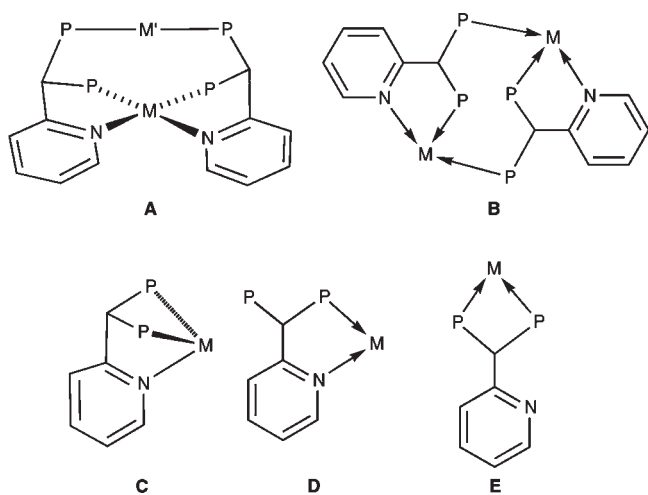
Received: December 9, 2010

Published: March 15, 2011

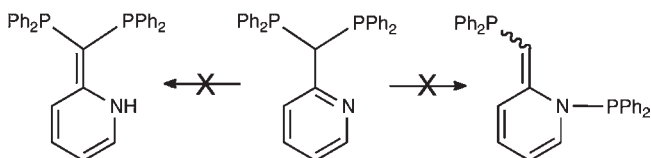
Scheme 1



Scheme 2. (Phenyl Groups Omitted)



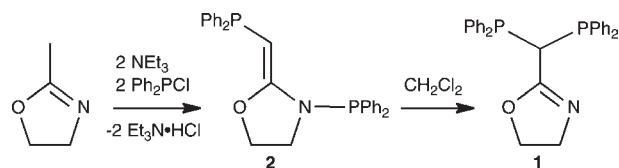
Scheme 3



preventing the tautomerisms shown in Scheme 3. Consistently and to the best of our knowledge, no H or PPh₂ shifts have been reported for this ligand.

In view of the coordination versatility of this class of ligands, and to extend studies performed with 2-{bis(diphenylphosphino)methyl}pyridine to another N-containing heterocycle, we have chosen to introduce an oxazoline moiety as a substituent on the PCP carbon. The oxazoline moiety with its N donor atom has been widely involved in *P,N*-chelating ligands for applications in, e.g., the catalytic oligomerization of ethylene and in asymmetric catalysis.⁸ However, the coordination behavior of 2-(bis(diphenylphosphino)methyl)-oxazoline ($(\text{Ph}_2\text{P})_2\text{CH}-\text{C}=\text{NCH}_2\text{CH}_2\text{O}$ (**1**)) has barely been studied.⁹ This geminal diphosphine ligand was prepared by the reaction of Ph₂PdCl and 2-methyl-2-oxazoline in the presence of NEt₃ and resulted from the rearrangement of the isomeric *P-C*, *P-N* diphosphine Ph₂PCH=COCH₂CH₂N(PPh₂) (**2**) (Scheme 4).⁹ The neutral Pt(II) complex [Pt{(Ph₂P)₂C···C(···NCH₂CH₂O)}₂] ([Pt(**1-H**)₂] (**3a**)), in which two deprotonated ligands **1-H** *P,P*-chelate the metal center, has been recently described.⁹

Scheme 4



The formation of **1** from **2** involves a *N* to *C* phosphoryl migration reaction. Related *N* to *C*¹⁰ and *C* to *N*¹¹ phosphoryl transfers have been observed recently. Phosphoryl migrations were also observed in several aminophosphine systems, showing, e.g., *P-N-N* to *N=P-N* rearrangements¹² and reversible *P-N-P* to *N=P-P* tautomerisms triggered by protonation/deprotonation of *N,N*-bis(diphenylphosphino)-pyridin-2-amine.¹³ *N* to *N* phosphoryl migrations were also reported,¹⁴ with one example concerning the Ni(II)-induced formation of a thiazoline-diphosphine sharing analogies with **2** and **2'** (see Scheme 10).¹⁵ Herein, we examine the coordination chemistry of ligand **1-H** with Pt(II) and Pd(II) precursors and describe some unexpected ligand rearrangements based on phosphoryl group migration. We shall also see that ligand **1-H** can exhibit both *P,N*- and *P,P*-chelating modes in the same compound.

RESULTS AND DISCUSSION

The Pd(II) complex [Pd{(Ph₂P)₂C···C(···NCH₂CH₂O)}₂] ([Pd(**1-H**),*P,P*]₂, **3b**), analogous to the Pt(II) complex **3a**, has been obtained by the reaction of **1** with [PdCl₂(NCPh)₂] in the presence of excess NEt₃. Complex **3b** can be obtained more conveniently by the reaction of **1** with [Pd(acac)₂], with the formation of acetylacetonate (see the Experimental Section). Excess ligand **1** with respect to palladium was used in these experiments to facilitate workup since **1** is very soluble in common organic solvents, in contrast to the Pd(II) precursor or the product. Purification of **3b** is facilitated by its poor solubility in MeCN, and the complex could be recrystallized from CH₂Cl₂/pentane as **3b**·4CH₂Cl₂ (Scheme 5, Figure 1).

Deprotonation of the free ligand **1** was not observed in the presence of NEt₃. This indicates that the formation of **3b** results from rapid deprotonation of a *P*- or *P,P*-coordinated intermediate. We shall see below that the Pt(II) bis-chelated complex **5** is indeed rapidly deprotonated by NEt₃ in MeCN.

In the structure of **3b** in **3b**·4CH₂Cl₂, the metal center is bis-chelated by two anionic **1-H** ligands, through the P atoms. The complex is centrosymmetric, resulting in a planar coordination geometry. The P1–Pd1–P2 chelating bite angle is 70.37(3)°, while the P1–C4–P2 angle is 100.30(16)°. The oxazoline ring is almost coplanar with the P1–C4–P2 group [angle between the mean planes: 2.41(1)°]. Although the C3–N1 distance is close to that expected for a double bond, the C3–C4 and C4–P separations are significantly shorter than typical C–C and C–P single bonds, suggesting significant electronic delocalization over the P1–P2–C4–C3–N1 group, consistent with the planar geometry around C4 [sum of the angles around C4: 359.7(6)°].

Bonding parameters in **3b** are consistent with the diphosphine and diphosphinomethanide limiting forms shown in Scheme 6, where the divalent character of the metal is retained. For simplicity, we will represent in the following the phosphorus–metal bonds involving this anionic ligand by simple lines.

This electronic delocalization is confirmed by a statistical analysis of the structural parameters retrieved from the 39

Scheme 5

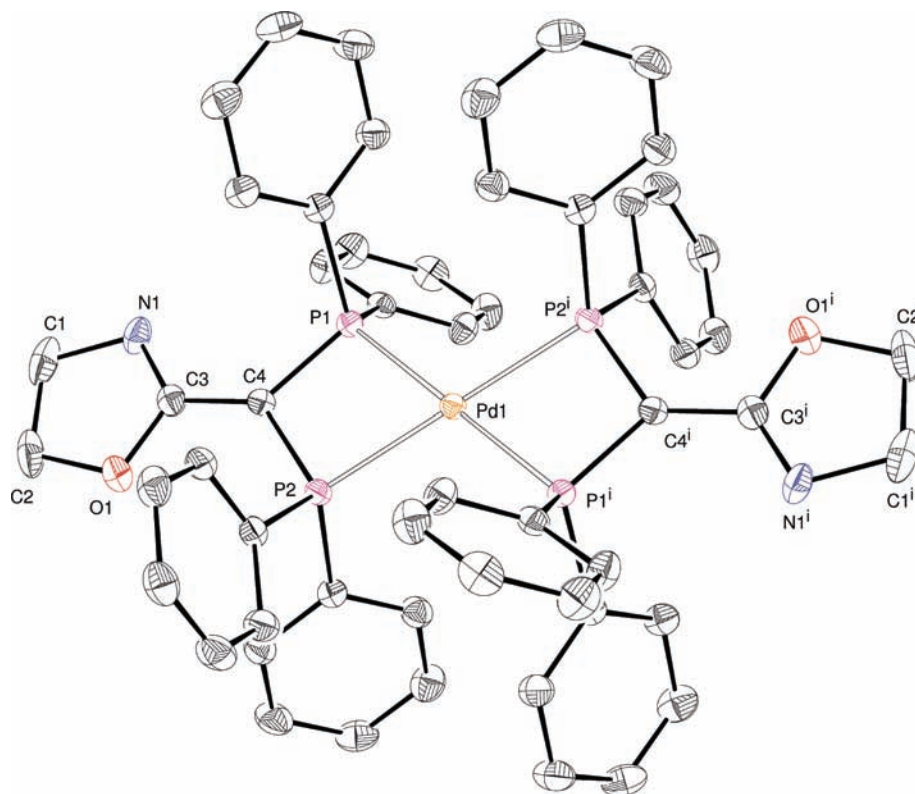
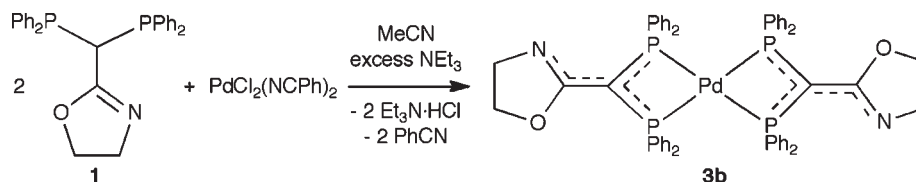
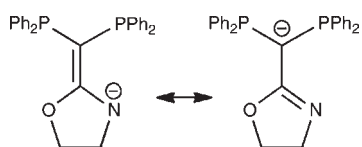


Figure 1. ORTEP of the molecular structure of **3b** in $3b \cdot 4CH_2Cl_2$. Hydrogen atoms and solvent molecules omitted for clarity. Ellipsoids include 40% of the electron density. Selected distances (Å) and angles (deg): Pd1–P2 2.3219(7), Pd1–P1 2.3391(7), P1–C4 1.748(3), P2–C4 1.751(3), N1–C3 1.291(4), N1–C1 1.475(4), C3–C4 1.432(4); P2–Pd1–P1 70.37(3), C4–P1–C5 114.65(13), C4–P1–Pd1 93.89(10), C4–P2–Pd1 94.41(10), C3–N1–C1 106.4(3), N1–C3–O1 117.9(3), N1–C3–C4 125.9(3), O1–C3–C4 116.1(3), C3–C4–P1 130.5(2), C3–C4–P2 128.9(2), P1–C4–P2 100.30(16).

Scheme 6. Limiting Mesomeric Forms of the 1-H Ligand



examples of chelating diphosphinomethanides of the type $R_2PC-(\cdots CR')PR_2$ (C = tricoordinated carbon). In the scatterogram reported in Figure 2, a clear correlation exists between the $C\cdots C$ bond length a and the $C-P$ separation b (correlation coefficient = -0.931).

The three longest $P-C$ bond lengths¹⁶ correspond to species in which CR' is an alkyl substituent, whereas in the samples showing the three shortest $P-C$ separations, CR' is a methylene¹⁷ or $C=CR'$ is an allene moiety.¹⁸ An intermediate situation

is observed in complex **3b**, similar to that found in complexes in which the substituent CR' contains a delocalized π system (e.g., aromatic imidazole¹⁹ or pyridine,^{2a,20} $-C(CO_2Me)=CH(CO_2Me)^{21}$). A recent example of a Pd(II) complex bischelated by substituted anionic dppm ligands featured a phosphonate group attached to the $P-C-P$ carbon.²²

In solution, the oxazoline protons give rise to two second-order triplets, whereas the $^{31}P\{^1H\}$ spectrum consists of a singlet at -28.9 ppm. The low ^{31}P multiplicity contrasts with the structure observed in the solid state, in which the phosphorus atoms within each ligand are nonequivalent. The presence of two different substituents (O and N) on C3 should formally lead to an $AA'BB'$ spin system for each ^{31}P nucleus. The singlet observed could result from accidental coincidence of the chemical shifts or from an equilibrium between the two possible C_{2v} and C_{2h} conformations of **3b** (not considering the phenyls) depicted in Scheme 7. This equilibrium may involve either

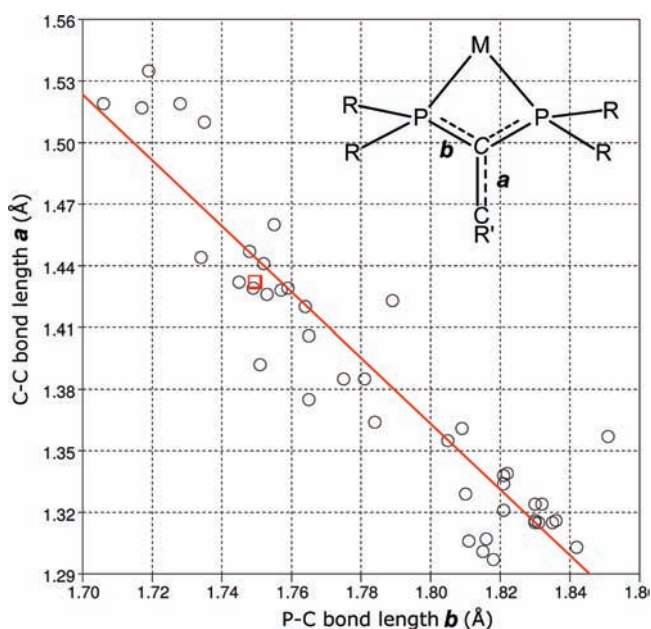
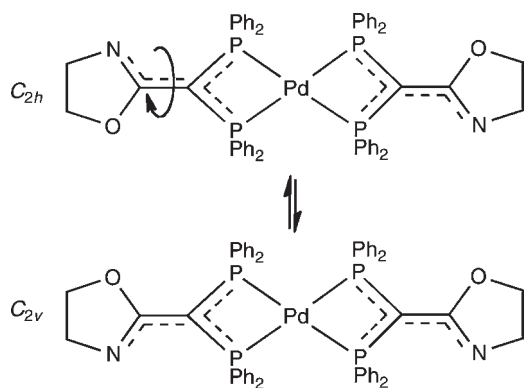


Figure 2. CSD scattergram correlating the C–C and C–P bond distances retrieved from the 39 examples of chelating diphosphines of the type $R_2PC(\cdots CR')PR_2$ (R = any C substituent, C = tricoordinated carbon, R' = any substituent) present in the CSD (Cambridge Structural Database). The regression line is depicted in red ($R = -0.931$), whereas the position of **3b** in the scattergram is represented with a red square.

Scheme 7



cleavage of a P–Pd bond with the formation of a tricoordinated intermediate, rotation about the remaining P–Pd bond and recoordination of the dangling P donor, or rotation about the C3–C4 bond while *P,P*-chelation is retained throughout the process. Although this bond shows partial double bond character, its length [1.432(4) Å, as observed in the X-ray structure] suggests a low rotation energy barrier. No splitting was observed upon cooling, suggesting that if this equilibrium exists, it is rapid on the NMR time scale. We shall see below (Scheme 12) an example where a similar dynamic behavior has been clearly evidenced.

In view of the availability of the oxazoline nitrogen donors for the stepwise construction of heterometallic complexes, we reacted **3b** with 2 equiv of $[AuCl(tht)]$ (tht = tetrahydrothiophene). Although the reaction resulted indeed in the quantitative formation of a trinuclear bimetallic complex, coordination of the Au(I) center did not occur at the nitrogen but at one of the

phosphorus groups initially bonded to Pd (Scheme 8). The molecular structure of this complex, $[Pd(1-H,P,N)_2(AuCl)_2]$ (**4**), was determined by single crystal X-ray diffraction methods (Figure 3).

In agreement with the spectroscopic results detailed below, the structure of **4** in $4 \cdot CHCl_3$ establishes that the originally *P,P*-chelating **1-H** ligands in **3b** now *P,N*-chelate the Pd atom, which is in a slightly distorted square planar environment. The second phosphorus atom of each ligand is coordinated to a AuCl group, with a typical linear coordination for this d^{10} metal center. Although they are not crystallographically related by symmetry, the two Pd(*P,N*) chelating moieties have very similar geometrical parameters. The Pd–P bonds are shorter in **4** than in **3b** [2.2756(18) Å and 2.2866(15) Å for **4** vs 2.3219(7) Å and 2.3391(7) Å for **3b**] as a result of the combined effect of their involvement in a five-membered vs a four-membered ring structure, respectively, and of the weaker *trans* influence of the nitrogen vs the phosphorus donor. The P–C–P angles are significantly wider than in **3b** [125.1(4)° and 122.9(4)° vs. 100.30(16)°], as a consequence of the relief of the four-membered rings' strain. The delocalization of the C=C partial double bond remains similar to that in **3b**, although the P–C–P carbons in the case of **4** display a slightly pyramidal environment (sum of the angles around C4 and C8: 356.5(13)° and 357.3(13)°, respectively). The $^{31}P\{^1H\}$ NMR spectrum of **4** consists of two doublets with shoulders (see Supporting Information, Figure S-1), well simulated by an $AA'XX'$ spin system with a geminal $^2J(P1,P3;P2,P4)$ coupling of ∓ 15.3 Hz, a *cis* $^2J(P1,P2)$ of ∓ 4.7 Hz, and a $^4J(P1,P4;P2,P3) = \pm 3.0$ Hz.

The rather slow (24 h reaction time) rearrangement of the ligand coordination mode on going from **3b** to **4** is thus preferred to the coordination of the nitrogen of **3b** to Au. The *P,N*-Pd, *P*-Au coordination modes comply well with the bonding preferences of the two metal centers, with the formation of stable P–Au–Cl and Pd(*P,N*)₂ arrangements. The *P,N*-chelating/*P,P*-bridging behavior of **1-H** observed in **4** is reminiscent of that of {2-(bis- R_2P)methylpyridines ($R = iPr, Ph$)}, which have led to a rich dinuclear chemistry.² Although the detailed mechanism of the ligand bonding rearrangement observed on going from **3b** to **4** is not established, we favor a metal-induced phosphorus migration from Pd to Au rather than a trapping by the Au(I) reagent of an intermediate with an already dissociated P donor. We note however that one of the chelating ligands in complex **8** (see below) displays a relevant bonding mode, but we never observed the formation of **8** directly from **3a**. A metal-induced rearrangement could be envisaged as being initiated by an interaction of the electrophilic gold(I) reagent with the electron-rich Pd(II) center followed by labilization of a P–Pd bond of the anionic four-membered *P,P*-chela. Interestingly, metal-promoted opening of the neutral four-membered *P,P*-chela in dppm complexes of Pd(II) and Pt(II) to form heterometallic complexes has been reported with nucleophilic carbonylmetalates.²³

Whereas **1** in excess reacted in acetonitrile with $[PtCl_2(NCPh)_2]$ in the presence of excess NEt_3 to give **3a**, the platinum analog of **3b**, two isomeric compounds were obtained when the same reaction was performed in the absence of a base (Scheme 9). The major isomer precipitated as $[Pt\{(Ph_2P)_2C=$
 $C(OCH_2CH_2NH)_2\}_2]Cl_2$ $[[Pt(I'-P,P)_2]Cl_2$, **5**, $I' = 2$ -(bis-(diphenylphosphino)methylene)oxazolidine, Scheme 9), whereas the minor product of this reaction was isolated from the acetonitrile

Scheme 8

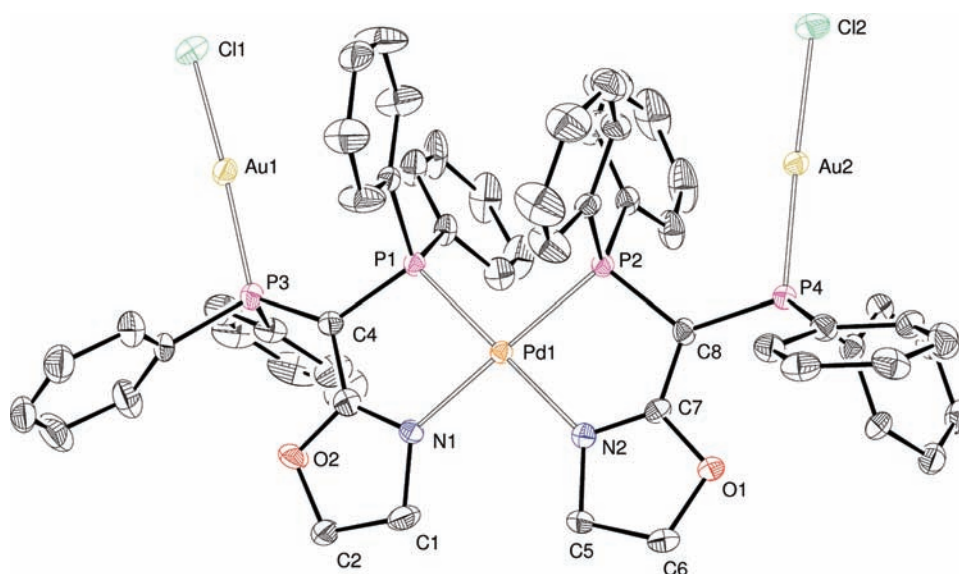
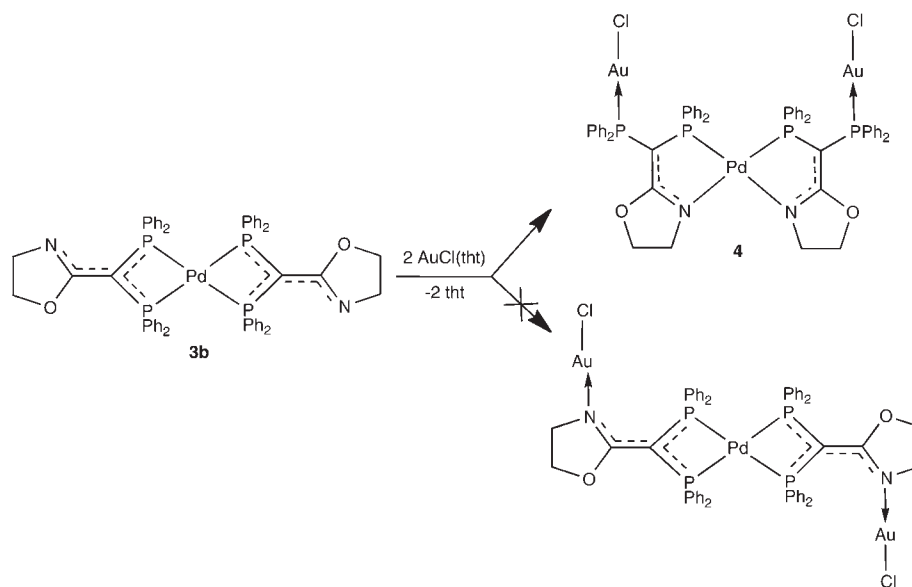


Figure 3. ORTEP of the molecular structure of **4** in $4 \cdot \text{CHCl}_3$. Hydrogen atoms and solvent molecules omitted for clarity. Ellipsoids include 50% of the electron density. Only one of the two similar independent molecules is shown. Selected distances (Å) and angles (deg): Au1–P3 2.2401(17), Au1–Cl1 2.2846(17), Au2–P4 2.2401(17), Au2–Cl2 2.2989(17), Pd1–N1 2.072(5), Pd1–N2 2.085(4), Pd1–P2 2.2756(18), Pd1–P1 2.2866(15), P1–C4 1.774(7), P3–C4 1.760(6), P2–C8 1.770(6), P4–C8 1.766(6), C3–C4 1.405(8), C7–C8 1.402(8), N1–C3 1.311(7), N2–C7 1.309(8); P3–Au1–Cl1 171.90(7), P4–Au2–Cl2 176.22(7), N1–Pd1–N2 96.8(2), N2–Pd1–P2 82.27(15), N1–Pd1–P1 82.91(14), P2–Pd1–P1 98.07(6), C3–C4–P3 120.7(5), C3–C4–P1 110.7(4), P3–C4–P1 125.1(4), N2–C7–O1 114.7(6), C7–C8–P2 111.4(4), P4–C8–P2 122.9(4), C7–C8–P4 124.6(4).

solution as $[\text{Pt}\{(\text{Ph}_2\text{P})_2\text{C}=\overline{\text{C}}(\text{OCH}_2\text{CH}_2\text{NH})\}\{\text{Ph}_2\text{PCH}=\overline{\text{C}}(\text{OCH}_2\text{CH}_2\text{N}(\text{PPh}_2))\}\text{Cl}_2]$ ($[\text{Pt}(\text{I}'\text{-}P,P)(\text{2}'\text{-}P,P)]\text{Cl}_2$, **6**, $2' = (E)$ -

3-(diphenylphosphino)-2-((diphenylphosphino)methylene)oxazolidine; Scheme 9). In compound **5**, the *P,P*-chelating ligand derives from **1** by a tautomeric H shift from C to N. Clearly, P coordination renders the C–H group more acidic. Complex **5** can be viewed as the dihydrochloride of **3a**, and it rapidly affords the latter when treated

with NEt_3 . Conversely, treatment of solid **3a** with aqueous HCl immediately results in the quantitative formation of **5**. Protonation of the oxazoline nitrogen atoms was indicated by ^1H NMR (CDCl_3) and by the disappearance of this signal in CD_3OD . Complex **6** could be crystallized as $6 \cdot 2.5\text{CH}_2\text{Cl}_2$ (Figure 4), and its structure was determined by X-ray diffraction methods.

In the crystals of **6** in $6 \cdot 2.5\text{CH}_2\text{Cl}_2$, two independent, isomeric molecules are present (see below), which display analogous bond distances and angles. The molecule not displayed

Scheme 9. Reactions in the Absence of Base

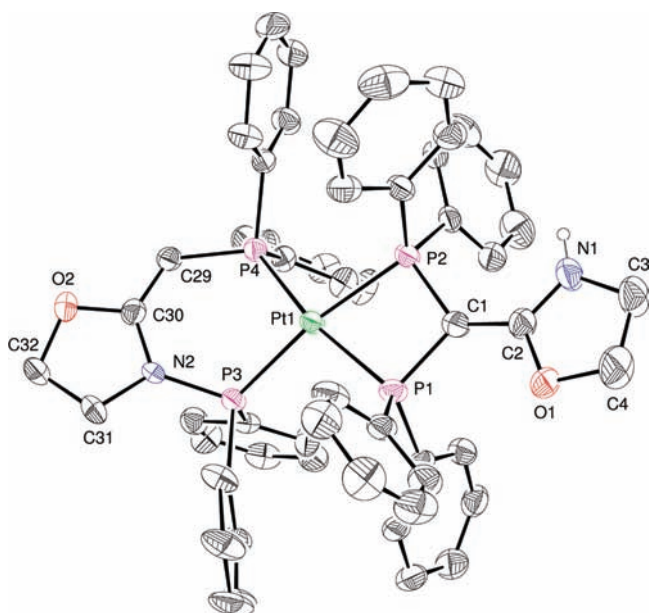
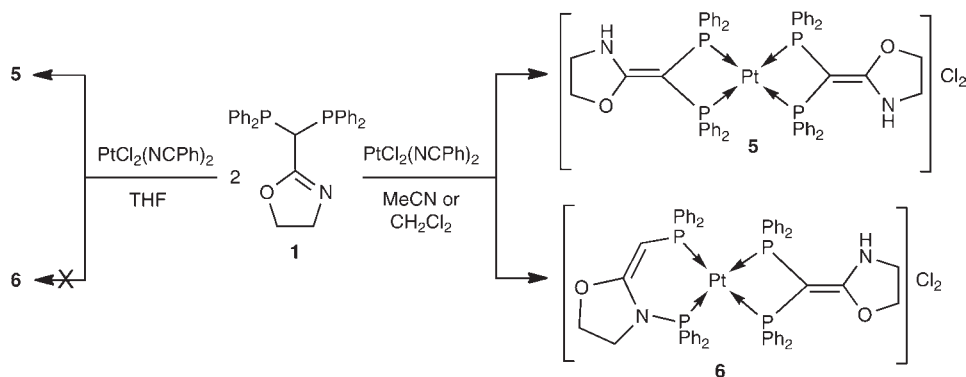


Figure 4. ORTEP of the molecular structure of the cation in $6 \cdot 2.5\text{CH}_2\text{Cl}_2$. One of the two independent molecules is depicted (see text). Hydrogen atoms and solvent molecules omitted for clarity. Ellipsoids include 40% of the electron density. Selected distances (Å) and angles ($^\circ$), molecule A: Pt1–P1 2.351(2), Pt1–P2 2.338(2), Pt1–P3 2.303(2), Pt1–P4 2.319(2), P1–C1 1.785(9), P2–C1 1.750(9), C1–C2 1.419(12), N1–C2 1.311(11), P3–N2 1.696(7), P4–C29 1.753(8), N2–C30 1.342(10), C29–C30 1.355(11); P2–Pt1–P1 71.51(8), P3–Pt1–P1 101.66(8), P4–Pt1–P2 99.53(7), P4–Pt1–P3 86.09(7), C1–P1–Pt1 92.4(3), C1–P2–Pt1 93.8(3), P2–C1–P1 101.6(5), P2–C1–C2 129.0(7), P1–C1–C2 127.1(7), N1–C2–C1 129.1(8), O1–C2–C1 117.7(9), N2–P3–Pt1 114.5(2), C29–P4–Pt1 114.7(3), C30–N2–P3 125.3(5), C30–C29–P4 127.1(6), N2–C30–C29 130.5(8), O2–C30–C29 119.1(7).

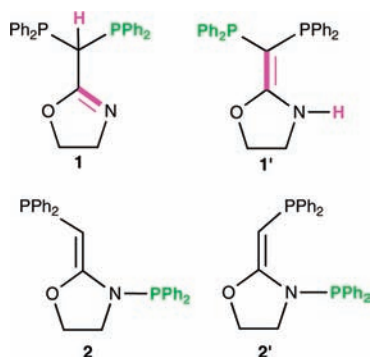
in Figure 4, is generated by a 180° rotation of the oxazoline ring about the C1–C2 bond. We shall see later that these two conformers are in equilibrium in solution. In both complexes of the asymmetric unit, the metal center is chelated by the ligand **1'**, (Scheme 10), through the P1 and P2 atoms, which leads to a four-membered chelate ring.

The slightly distorted square-planar coordination sphere of the metal in **6** is completed by the P–C, P–N diphosphine **2'**, (Scheme 10), which binds to the metal through the two P donors and leads to a six-membered ring (Pt1, P3, N2, C30, C29,

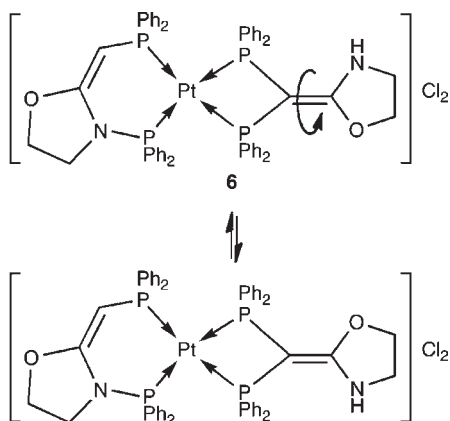
P4; Figure 4). In ligand **1'**, the double bond is formally localized between C1 and C2 (Scheme 10). However, the C1–C2 [1.419(12) Å], C2–N1 [1.311(11) Å], P1–C1 [1.785(9) Å], and P2–C1 [1.750(9) Å] distances in **6** suggest an electronic delocalization similar to that encountered in **3b**. This results in a planar environment around the C1 atom [sum of the angles around C1: $358(2)^\circ$]. Ligand **2'** is the *E* isomer of diphosphine **2** (Scheme 10), with respect to the C29=C30 double bond. Only the *Z* isomer **2** has been isolated before, and it was found to be an intermediate in the formation of **1** (Scheme 4),⁹ as a result of N to C phosphoryl migration. The bond parameters within the P4–C29–C30–N2–P3 group in **6** are significantly different from those in the free ligand **2**. The C29–C30 distance [1.355(11) Å] in **6** is longer than the corresponding C–C bond [1.332(5) Å] in **2**, while the N2–C30 bond [1.342(10) Å] in **6** is shorter than that in **2** [1.391(5) Å]. The P3–N2 [1.696(7) Å] and P4–C29 [1.753(8) Å] bonds are both shorter than those in **2** [P–N 1.718(3) Å, P–C 1.784(4) Å],⁹ which corresponds to a more significant delocalization of the double bond over the P4–C29–C30–N2–P3 group in **6**.

Complexes **5** and **6** have been characterized in solution by NMR spectroscopy. In the $^{31}\text{P}\{^1\text{H}\}$ NMR spectrum of **5**, the phosphorus atoms resonate at -33.7 ppm, with a $^1J(^{31}\text{P}, ^{195}\text{Pt})$ coupling constant of 1980 Hz, which is consistent with the *trans* influence of a P donor. In the ^1H NMR (CDCl_3) spectrum, the NH protons resonate at 10.11 ppm, and this signal disappears in CD_3OD due to the H/D exchange process. The $^{31}\text{P}\{^1\text{H}\}$ spectrum of **6** (see Supporting Information, Figure S-2) is fully consistent with its X-ray structure (Figure 4). The four phosphorus atoms, as expected for an ABXY spin system, resonate as four ddd with ^{195}Pt satellites [2637 Hz (P3), 2302 Hz (P4), 2155 Hz (P2), 2044 Hz (P1)]. The largest $^1J(\text{P}, \text{Pt})$ is found for P3, and this could be due to the higher electronegativity of the N substituent.²⁴ As expected, the largest P,P coupling constants (see Table 1) correspond to nuclei in a mutual *trans* arrangement [$^2J(\text{P}2, \text{P}3)$ and $^2J(\text{P}1, \text{P}4)$, 370 and 314 Hz, respectively]. The relatively high coupling constant $J(\text{P}3, \text{P}4)$ of 38 Hz for P nuclei in a *cis* arrangement probably involves a “through ligand” $^4J(\text{P}3, \text{P}4)$ contribution. In the ^1H NMR spectrum, the NH proton resonates at 8.6 ppm, while the olefinic CH gives rise to a doublet of doublets at 4.13 ppm, due to coupling with P3 [$^4J(\text{H}, \text{P}3) = 3.6$ Hz] and P4 [$^2J(\text{H}, \text{P}4) = 6.8$ Hz].

At temperatures below -10°C , splitting of the ^{31}P signals was observed for **6**, consistent with an equilibrium involving rotation of the oxazoline ring about the C1–C2 bond (Scheme 11), similar to that envisaged for **3b** (Scheme 7). The broad and

Scheme 10. Tautomeric/Isomeric Forms of the Diposphine–Oxazoline System

Table 1. P–Pt–P Angles and Corresponding P,P Coupling Constants in the $^{31}\text{P}\{^1\text{H}\}$ NMR Spectrum of **6**

	angles (deg)	coupling constants (Hz)
P1–Pt1–P4	167.71(8)	$^2j(\text{P1,P4}) = 314$
P2–Pt1–P3	170.20(8)	$^2j(\text{P2,P3}) = 370$
P1–Pt1–P2	71.51(8)	$^2j(\text{P1,P2}) = 15$
P1–Pt1–P3	101.66(8)	$^2j(\text{P1,P3}) = 11$
P2–Pt1–P4	99.53(7)	$^2j(\text{P2,P4}) = 10$
P3–Pt1–P4	86.09(7)	$^4j(\text{P3,P4}) = 38$

Scheme 11


overlapping signals observed at room temperature became sharp at a higher temperature (50 °C, estimated $\Delta G^\ddagger = 61 \pm 1 \text{ kJ} \cdot \text{mol}^{-1}$). In agreement with an increased double bond character for C1–C2 in **6** with respect to C3–C4 in **3b**, a higher ΔG^\ddagger value is found for this phenomenon in **6**.

In the reaction of **1** with $[\text{PtCl}_2(\text{NCPH})_2]$ leading to **6**, it is unlikely that residual **2** in solution could be responsible for the formation of coordinated **2'**. Ligand **2** is a thermally unstable and sensitive compound, which easily and quickly undergoes cleavage of the P–N bond to form the monophosphine- $\text{Ph}_2\text{PCH}_2\text{C}=\text{NCH}_2\text{CH}_2\text{O}$.⁹ Furthermore, reaction of pure **2** with $[\text{MCl}_2(\text{NCPH})_2]$ (M = Pt(II), Pd(II)) results in its degradation and leads to the formation of various complexes containing $\text{Ph}_2\text{PCH}_2\text{C}=\text{NCH}_2\text{CH}_2\text{O}$. Since **2'** has never been observed,

even spectroscopically, as free diposphine, its stability is suggested to be even lower than that of **2**. The stabilization of **2'** upon coordination to a metal center is noteworthy, since complex **6** is thermally stable and does not readily undergo hydrolysis or alcoholysis.

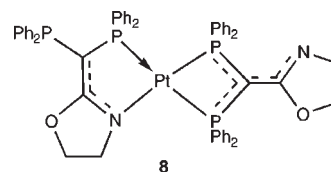
It is thus most likely that the **1**→**2'** isomerization is metal-promoted, possibly through a pentacoordinated intermediate (Scheme 12).

Indeed, an isoelectronic Rh(I) complex showing a connectivity similar to that of hypothetical intermediate **A** in Scheme 12 has been described, namely, $[\text{Rh}\{P,P,N-(\text{Ph}_2\text{P})_2\text{CH}_2\text{-2-Py}\}(\text{NBE})](\text{BF}_4)$.⁶ In this complex, a 2-pyridine-functionalized diposphine similar to **1** acts as a tricoordinating, facial ligand and the environment of its P–C–P carbon shows a significant distortion from the ideal tetrahedral geometry. Intermediate **A** would then isomerize *via* insertion of one of the phosphoryl groups into the Pt–N bond, with the formation of **6**. A tetracoordinated intermediate (**B**), possibly in equilibrium with **A**, would instead give **5** *via* 1,3 proton transfer.

Diposphines **1**, **1'**, and **2/2'** represent the possible phosphoryl/H tautomers involving the exocyclic carbon and the nitrogen of the bis(diphenylphosphino)oxazoline system. Related imino/amino tautomerisms involving a N to N proton exchange between the exo- and endocyclic nitrogens were observed in a system containing 2-amino-oxazoline²⁵ and 2-amino-thiazoline.²⁶

The formation of **6** was found to be solvent-dependent, since when the reaction of 2.3 equiv of **1** with $[\text{PtCl}_2(\text{NCPH})_2]$ was performed in THF, it did not give **6**, but complex **5** was instead obtained quantitatively, whereas in MeCN or CH_2Cl_2 , a mixture of **5** and **6** was obtained (Scheme 9). NMR monitoring in CDCl_3 showed that in the presence of excess NEt_3 , **6** is mono-deprotonated within a few minutes upon scavenging of the oxazoline NH proton to give rise to $[\text{Pt}(1\text{-H-P,P})(2'\text{-P,P})]\text{Cl}$ (**7**, Scheme 13) in spectroscopic quantitative yields ($^{31}\text{P}\{^1\text{H}\}$ NMR in CDCl_3). The signals of the P3 (50.9 ppm) and P4 (−4.3 ppm) nuclei are slightly shifted when compared to those of **6** (2 ppm highfield and 1.5 ppm lowfield, respectively), while those of the former P1 and P2 did not shift significantly. In the ^1H NMR spectrum, as expected, the NH proton signal disappeared (see Supporting Information, Figure S-3).

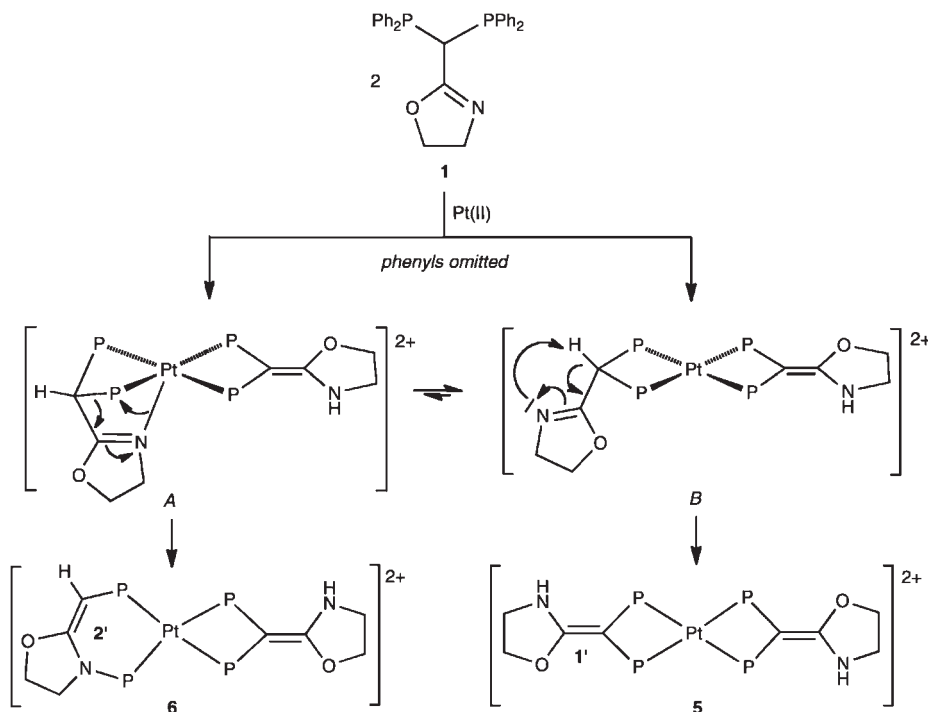
However, when the reaction between excess **1** and $[\text{PtCl}_2(\text{NCPH})_2]$ in CH_2Cl_2 was performed in the presence of excess triethylamine, small amounts of $[\text{Pt}(1\text{-H-P,P})(1\text{-H-P,N})]$ (**8**) were obtained, along with isomeric **3a**, the major product of this reaction.



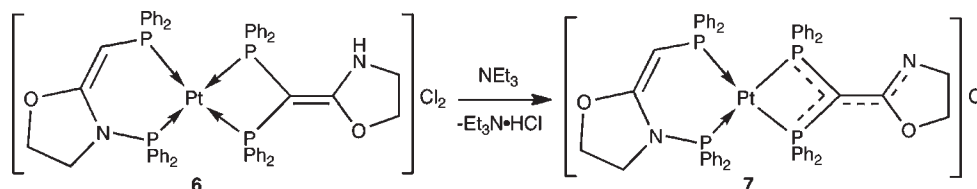
The crystal structure of **8** in $8 \cdot \text{CH}_2\text{Cl}_2$ was determined by X-ray diffraction (Figure 5).

In the structure of **8** in $8 \cdot \text{CH}_2\text{Cl}_2$, the Pt(II) center shows a square-planar coordination geometry. The metal center is bis-chelated by two **1-H** ligands, one chelating through the P1 and P2 atoms, while the second **1-H** ligand displays a P,N-coordination mode (through P3 and N2). One of the PPh₂ groups of the P,N chelating diposphine is thus not coordinated. The Pt–P1 bond [2.2704(14) Å] is shorter than Pt–P2 [2.3199(16) Å]

Scheme 12



Scheme 13



and Pt–P3 [2.3219(15) Å], consistent with the weaker *trans* influence of the nitrogen vs the phosphorus donor. The P1–C1–P2 angle [99.2(3)°], within the four-membered ring, is dramatically smaller than the P3–C29–P4 [121.2(3)°] angle. The double bond in the *P,N*-chelate is highly delocalized, the N2–C30 [1.333(7) Å] and C29–C30 [1.388(8) Å] separations being intermediate between those expected for N–C and C–C single and double bonds, respectively. The *P,P*-chelating diphosphine shows a bonding situation similar to that observed in 3a. The anionic chelating ligands in 8 illustrate the limiting forms of ligand 1 (Scheme 6). Although the existence of 4 suggests that a complex containing two *P,N*-chelating ligands resulting from deprotonation of a type 1' ligand is sterically possible, as also indicated by the characterization of Pd(II) and Pt(II) complexes with closely related *P,N*-chelates,^{26,27} we did not observe the formation of such a complex, either upon thermal treatment of 8 or in the course of the reactions reported herein.

The formation of 8 depends on the order in which the reagents are added. When the Pt(II) precursor complex was added to a solution of 1 and NEt₃, the formation of 3a and 8 was observed, whereas the addition of NEt₃ to a solution mixture of [PtCl₂-(NPh)₂] and 1 resulted instead in the rapid formation of 3a and 7. Independently, solutions of complexes 3a, 5, or 6 did not

afford 8 upon thermal treatment (in MeCN, CH₂Cl₂, acetone, or solid) or reaction with NEt₃ (in MeCN or CH₂Cl₂), respectively. These data suggest that 8 stems from an intermediate that is too rapidly deprotonated to form 7 via 6. We can thus assume that the presence of NEt₃ in CH₂Cl₂, when the precursor is added, would prevent the formation of a cationic intermediate of type A (Scheme 12) leading to 6.

The structure of 8 is retained in solution, as indicated by its ³¹P{¹H} NMR spectrum, which consists of four groups of signals corresponding to the four chemically different phosphorus nuclei (see Supporting Information, Figure S-4). The assignment of the P4 signal is facilitated by its small coupling with ¹⁹⁵Pt (87 Hz), consistent with typical ³J(P,Pt) values found in the literature.²⁸ The coupling constants are summarized in Table 2 and compared to those observed in 4.

Although the structural parameters of the P3–C29–P4 group are similar to those in 4, including the P–C–P angles [121.2(3)° in 8, 125.1(4) and 122.9(4)° in 4] and the P–C bond distances [1.765(6) and 1.781(6) Å for P3–C29 and P4–C29 in 8; 1.770(6) and 1.766(6) Å for P2–C8 and P4–C8 in 4], the ²J(P3,P4) of 81 Hz is much larger than that in ²J(P1,P3) or ²J(P2,P4) in 4 (15.3 Hz), suggesting that the absolute value of the coupling constants is influenced by the significant

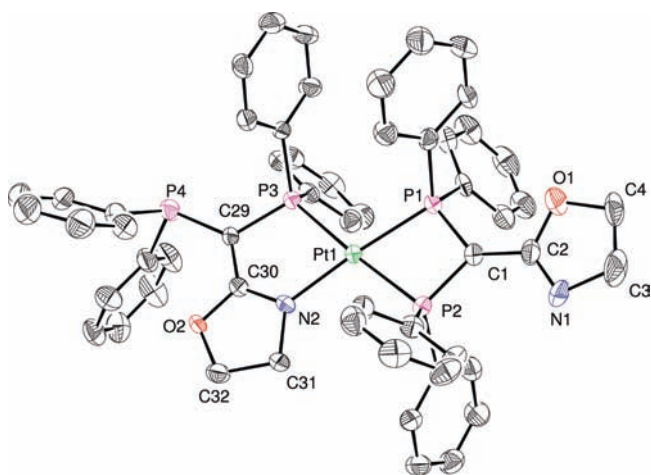
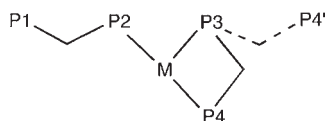


Figure 5. ORTEP of the molecular structure of **8** in $8 \cdot \text{CH}_2\text{Cl}_2$. Hydrogen atoms and solvent molecules omitted for clarity. Ellipsoids include 40% of the electron density. Selected distances (Å) and angles (deg): Pt1–P1 2.2704(14), Pt1–P2 2.3199(16), Pt1–P3 2.3219(15), Pt1–N2 2.048(4), P1–C1 1.745(6), P2–C1 1.758(6), C1–C2 1.432(8), N1–C2 1.289(8), P3–C29 1.765(6), P4–C29 1.781(6), N2–C30 1.333(7), C29–C30 1.388(8); P2–Pt1–P1 71.05(6), P1–Pt1–P3 105.26(5), N2–Pt1–P3 80.93(13), N2–Pt1–P2 102.83(14), C1–P1–Pt1 95.90(19), C1–P2–Pt1 93.8(2), P1–C1–P2 99.2(3), N1–C2–C1 125.9(6), C29–P3–Pt1 114.2(2), C30–N2–Pt1 119.5(4), N2–C30–C29 125.6(5), O2–C30–C29 120.9(5), P3–C29–P4 121.2(3).

Table 2. Comparison of the $J(\text{P},\text{P})$ Coupling Constants in **8** and **4**, Together with a Common Atoms Numbering Scheme (Phenyls, Oxazoline Rings, and AuCl Groups of **4** Omitted; $\text{M} = \text{Pt}$ in **8** and $\text{M} = \text{Pd}$ in **4**; P4 for **8** and P4' for **4**)



	coupling in 8 (Hz)	coupling in 4 (Hz)
$J(\text{P1},\text{P2})$	81	15
$J(\text{P1},\text{P3})$	0	3
$J(\text{P1},\text{P4})$	17	
$J(\text{P1},\text{P4}')$		0
$J(\text{P2},\text{P3})$	4	5
$J(\text{P2},\text{P4})$	346	
$J(\text{P2},\text{P4}')$		3
$J(\text{P3},\text{P4})$	9	
$J(\text{P3},\text{P4}')$		15

electronic effect exerted by the P-coordinated AuCl group.²⁴ Noteworthy is the rather large *transoid* 4J coupling of 17 Hz between P2 and P4.

CONCLUSION

Ligand **1** has proven to be an efficient multidentate ligand with a rich coordination chemistry involving diverse ligand rearrangements. Among the four formula isomeric ligands **1**, **1'**, **2**, and **2'**, **1** and **2** are stable as free ligands whereas **1'** and **2'** need to be

stabilized by metal coordination (Scheme 10). Differently from systems such as 2{bis(diphenylphosphino)methyl}pyridine in which the nitrogen atom is part of an aromatic ring, deprotonation of the P–C–P carbon takes place without the use of a base as a result of the basicity of the oxazoline N donor (complex **5**). Deprotonation of the resulting NH function can occur with retention of the *P,P*-chelation mode of the ligand or trigger formation of *P,N*-chelates. Complexes have been characterized in which ligand **1**_H showed three different coordination modes, namely, *P,P*-chelating (**3b**), *P,N*-chelating (**8**), and *P,N/P,P*-chelating/bridging (**4**). This emphasizes the versatility of this functional ligand. The phosphoryl migration reaction leading to **6** represents a rare case of C→N phosphoryl tautomerism. The various ligand rearrangements and bonding modes encountered in the course of this work are summarized in Scheme 14. This diversity will allow further developments.

Complexes **3a** and **3b** are luminescent, probably because of the electronic delocalization over the ligand backbone in **1**_H. As mentioned above, this delocalization can be tuned by linking different functionalities to the P–C–P carbon center. The photophysical properties of these and related complexes are under investigation.

EXPERIMENTAL SECTION

General Considerations. All manipulations were carried out under an inert argon atmosphere, using standard Schlenk-line conditions and dried and freshly distilled solvents. Unless otherwise stated, the ^1H , $^{13}\text{C}\{^1\text{H}\}$, and $^{31}\text{P}\{^1\text{H}\}$ NMR spectra were recorded on a Bruker Avance 300 instrument at 300.13, 75.47, and 121.49 MHz, respectively, using TMS or H_3PO_4 (85% in D_2O) as external standards, with downfield shifts reported as positive. All NMR spectra were measured at 298 K, unless otherwise specified. The assignment of the signals was made by ^1H , ^1H -COSY, ^1H , ^{13}C -HMQC, and ^{13}C -HSQC experiments. Elemental C, H, and N analyses were performed by the “Service de micro-analyses”, Université de Strasbourg. $[\text{PtCl}_2(\text{NCPH})_2]$, $[\text{PdCl}_2(\text{NCPH})_2]$,²⁹ $[\text{AuCl}(\text{tht})]$ ³⁰ (tht = tetrahydrothiophene), complex **3a**, and ligand **1**⁹ were prepared according to literature procedures. $\text{Ph}_2\text{P}\text{Cl}$ and NEt_3 were freshly distilled before use. Other chemicals were commercially available and were used as received.

Preparation and Spectroscopic Data for $[\text{Pd}(\mathbf{1}_{\text{H}}\text{-P},\text{P})_2]$ (3b**)**

a. Pure NEt_3 (0.50 mL, 3.59 mmol) was added to a stirred solution of ligand **1** (0.530 g, 1.17 mmol) in MeCN (50 mL), and solid $[\text{PdCl}_2(\text{NCPH})_2]$ (0.150 g, 0.39 mmol) was added. The solution was stirred for 3 h, whereupon an orange precipitate formed. The solid was collected by filtration and washed with MeCN (2×20 mL) and Et_2O (10 mL). Evaporation of the volatiles afforded compound **3b** as an orange powder. Yield: 0.191 g, 48%, based on Pd. The product can be recrystallized by layering pentane onto a solution of **3b** in CH_2Cl_2 . ^1H NMR (CDCl_3): 3.57 (2nd order t, 4H, $^3J(\text{H},\text{H}) = 8.7$ Hz, NCH_2), 3.80 (2nd order t, 4H, $^3J(\text{H},\text{H}) = 8.7$ Hz, OCH_2), 7.03–7.45 (m, 40H, Ph). $^{31}\text{P}\{^1\text{H}\}$ NMR (CDCl_3): –28.9 (s). $^{13}\text{C}\{^1\text{H}\}$ NMR (CDCl_3): 30 (br, P–C–P), 54.6 (br, NCH_2), 65.7 (s, OCH_2), 128.0–134.5 (m, Ph), 165.2 (s, O–C=N). Anal. Calcd for **3b**· CH_2Cl_2 (1096.24): C, 62.45; H, 4.60; N, 2.56. Found: C, 61.96; H, 4.63; N, 2.47.

b. Solid $[\text{Pd}(\text{acac})_2]$ (0.100 g, 0.33 mmol) was added to a stirred solution of ligand **1** (0.400 g, 0.88 mmol) in THF. The reaction mixture was stirred for 12 h, whereupon an orange precipitate formed. This solid was collected by filtration and washed with THF (2×10 mL) and Et_2O (2×10 mL). Evaporation of

Scheme 14

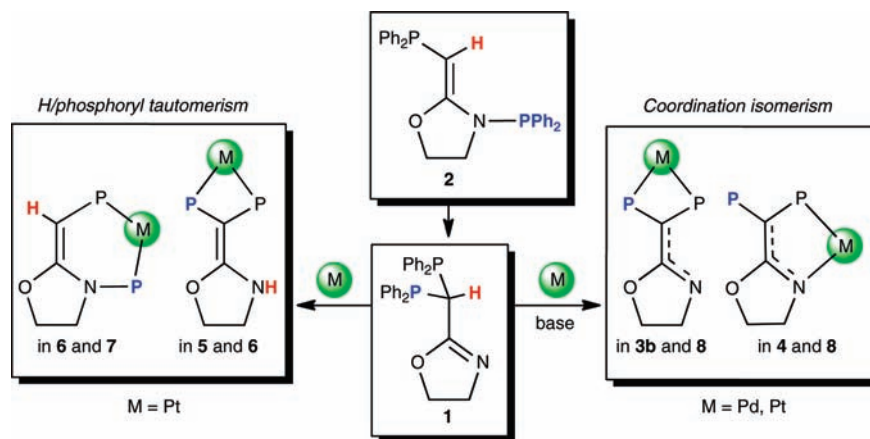


Table 3. X-Ray Data Collection and Refinement Parameters

compound	3b · 4CH ₂ Cl ₂	4 · CHCl ₃	6 · 2.5CH ₂ Cl ₂	8 · CH ₂ Cl ₂
chemical formula	C ₅₆ H ₄₈ N ₂ O ₂ P ₄ Pd · 4(CH ₂ Cl ₂)	C ₅₆ H ₄₈ Au ₂ Cl ₂ N ₂ O ₂ P ₄ Pd · CHCl ₃	C ₅₆ H ₅₀ Cl ₂ N ₂ O ₂ P ₄ Pt · 2.5(CH ₂ Cl ₂)	C ₅₇ H ₅₀ Cl ₂ N ₂ O ₂ P ₄ Pt · CH ₂ Cl ₂
formula mass	1350.95	1595.45	1385.16	1184.86
crystal syst	triclinic	monoclinic	triclinic	monoclinic
a/Å	9.8705(5)	25.1972(4)	17.0905(5)	18.8057(5)
b/Å	12.5788(5)	24.7389(5)	18.0349(8)	12.9167(2)
c/Å	13.3436(6)	18.8381(4)	24.3921(10)	26.3580(6)
α/deg	75.682(2)	90.00	107.918(2)	90.00
β/deg	73.222(2)	107.4140(10)	107.738(2)	128.311(2)
γ/deg	74.038(2)	90.00	90.299(3)	90.00
unit cell volume/Å ³	1499.46(12)	11204.5(4)	6772.8(5)	5023.8(2)
temperature/K	173(2)	173(2)	173(2)	173(2)
space group	P $\bar{1}$	P2 ₁ /c	P $\bar{1}$	P2 ₁ /c
Z	1	8	4	4
abs coeff, μ/mm ⁻¹	0.817	5.939	2.480	3.072
M	15842	94803	38965	20068
indep reflns	6862	25553	27358	11501
R _{int}	0.0693	0.0709	0.0364	0.0454
R ₁ (I > 2σ(I))	0.0474	0.0464	0.0656	0.0417
wR(F ²) (I > 2σ(I))	0.1014	0.0944	0.1677	0.0921
R ₁ (all data)	0.0712	0.1137	0.1238	0.0853
wR(F ²) (all data)	0.1107	0.1147	0.1859	0.1324
goodness of fit on F ²	1.033	1.006	0.952	0.989
no. of params	349	1315	1342	631

the volatiles afforded **3b** as an orange powder. Yield: 0.305 g, 92% based on Pd.

Preparation and Spectroscopic Data for [Pd(1-*H*-P,N)₂(AuCl)₂] (4). Solid [AuCl(tht)] (0.032 g, 0.10 mmol) was added to a stirred solution of **3b** (0.050 g, 0.049 mmol) in CH₂Cl₂ (20 mL). Stirring was continued for 24 h. The volatiles were removed under vacuum conditions, and the residue was washed with diethyl ether (2 × 10 mL) and dried under reduced pressure to give compound **4** as a yellow powder. Yield: 0.056 g, 77%. The product was recrystallized by layering a CH₂Cl₂ solution of **4** with pentane. ¹H NMR (CDCl₃): 3.90 (2nd order triplet, 4H, ³J(H,H) = 8.1 Hz, NCH₂), 4.17 (2nd order triplet, 4H, ³J(H,H) = 8.1 Hz, OCH₂), 6.98–7.60 (m, 40H, Ph). ³¹P{¹H}

NMR (CDCl₃): AA'BB' spin system, 13.9 (d with satellites, simulated, ²J(P^B,P^{B'}) = 5 Hz, ²J(P^A,P^B) = 15 Hz, ⁴J(P^A,P^{B'}) = -3 Hz, P^A-Au), 34.0 (d with satellites, simulated, ²J(P^B,P^{B'}) = 5 Hz, ²J(P^A,P^B) = 15 Hz, ⁴J(P^A,P^{B'}) = -3 Hz, P^B-Pd). ¹³C{¹H} NMR (CDCl₃): 40.8 (pseudo t, ¹J(C,P) = 67 Hz, P-C-P), ³¹ 52.3 (s, NCH₂), 69.5 (s, OCH₂), 127.7–133.2 (m, Ph), 180.5 (dd, J(C,P) = 41.8 and 1.7 Hz, O-C-N). Anal. Calcd for 4 · CH₂Cl₂ (1561.08): C, 43.85; H, 3.23; N, 1.79. Found: C, 43.39; H, 3.28; N, 1.62.

Preparation and Spectroscopic Data for [Pt(1'-P,P)₂]Cl₂ (5) and [Pt(1'-P,P)(2'-P,P)]Cl₂ (6)

a. When solid [PtCl₂(NPh)₂] (0.400 g, 0.85 mmol) was added to a stirred solution of ligand **1** (0.900 g, 1.98 mmol) in

MeCN (50 mL), rapid precipitation of a colorless powder occurred, and stirring was continued for 1 h. The solid was collected by filtration and washed with MeCN (2×10 mL), giving **5** as a colorless powder after evaporation of the volatiles. Yield: 0.690 g, 69%. The filtrate was combined with the acetonitrile washing fractions and dried under vacuum conditions, affording a yellow viscous residue to which THF (30 mL) was added. The resulting suspension was stirred for 3 h, and the precipitate was collected by filtration and redissolved in a minimum amount of MeCN. To this solution, Et₂O was added (200 mL), affording **6** as a colorless powder, which was collected by centrifugation and dried under vacuum conditions. Yield: 0.250 g, 25%. Crystals of $6 \cdot 2.5\text{CH}_2\text{Cl}_2$ were obtained by layering pentane onto a saturated solution of **6** in CH₂Cl₂.

b. When solid [PtCl₂(NPh)₂] (0.200 g, 0.42 mmol) was added to a stirred solution of ligand **1** (0.500 g, 1.10 mmol) in THF (50 mL), rapid precipitation of a colorless powder occurred, and stirring was continued for 1 h. The solid was collected by filtration and washed with THF (2×10 mL), giving **5** as a colorless powder after evaporation of the volatiles. Yield: 0.478 g, 96%.

Compound **5**. ¹H NMR (CDCl₃): 3.67 (2nd order triplet, 4H, ³J(H,H) = 8.7 Hz, NCH₂), 4.10 (2nd order triplet, 4H, ³J(H,H) = 8.7 Hz, OCH₂), 7.13–7.36 (m, 40H, Ph), 10.11 (br, NH). ³¹P{¹H} NMR (CDCl₃): –33.7 (s, with Pt satellites, ¹J(P,Pt) = 1980 Hz). ¹³C{¹H} NMR (CD₃OD): 45.5 (s, NCH₂), 58.4 (t, ¹J(C,P) = 30 Hz, P–C–P), 71.3 (s, OCH₂), 130.7–134.2 (m, Ph), 171.5 (s, with ¹⁹⁵Pt satellites, ³J(C,Pt) = 42 Hz, O–C=N). Anal. Calcd for **5** (1172.89): C, 57.35; H, 4.30; N, 2.39. Found: C, 56.80; H, 4.10; N, 2.16.

Compound **6**. Assignments refer to Figure 4. ¹H NMR (CD₃CN): 3.32 (t, 2H, ³J(H,H) = 7.4 Hz, N₂CH₂), 3.38 (t, 2H, ³J(H,H) = 8.7 Hz, N₁CH₂), 4.12 (t, 2H, ³J(H,H) = 8.7 Hz, O₁CH₂), 4.13 (dd, 1H, ²J(H,P) = 6.8 Hz, ⁴J(H,P) = 3.6 Hz, values determined by ¹H HMQC, H29), 4.29 (t, 2H, ³J(H,H) = 7.4 Hz, O₂CH₂), 6.87–7.78 (m, 40H, Ph), 8.60 (br, 1H, NH). ³¹P{¹H} NMR (CD₃CN) (see Figure 4 for labeling): –38.9 (ddd, with Pt satellites, ²J(P₂,P₄) = 10 Hz, ²J(P₂,P₁) = 15 Hz, ²J(P₂,P₃) = 370 Hz, ¹J(P,Pt) = 2155 Hz, P₂), –38.0 (ddd, with Pt satellites, ²J(P₁,P₃) = 11 Hz, ²J(P₁,P₂) = 15 Hz, ²J(P₁,P₄) = 314 Hz, ¹J(P,Pt) = 2044 Hz, P₁), –2.8 (ddd, with Pt satellites, ²J(P₄,P₂) = 10 Hz, ²⁺⁴J(P₄,P₃) = 38 Hz, ²J(P₄,P₁) = 314 Hz, ¹J(P,Pt) = 2302 Hz, P₄), 49.6 (ddd, with Pt satellites, ²J(P₃,P₁) = 11 Hz, ²⁺⁴J(P₃,P₄) = 38 Hz, ²J(P₃,P₂) = 370 Hz, ¹J(P,Pt) = 2637 Hz, P₃). ¹³C{¹H} NMR (CD₃CN): 45.3 (s, C₃), 51.4 (s, C₃₁), 57.1 (t, ¹J(C,P) = 58 Hz, C₁), 60.1 (ddd, ¹J(C,P₄) = 81 Hz, ³J(C,P) = 5.5 and 2.5 Hz, C₂₉), 67.2 (d, ³J(C,P) = 6.0 Hz, C₃₂), 70.2 (s, C₄), 128.8–135.6 (m, Ph), 165.9 (dd, ²J(C,P) = 18.5 and 12.8 Hz, C₃₀), 168.9 (t, with ¹⁹⁵Pt satellites, ²J(C,P) = 4.2 Hz, ³J(C,Pt) = 98 Hz, C₂). Anal. Calcd for **6** (1172.89): C, 57.35; H, 4.30; N, 2.39. Found: C, 57.30; H, 4.34; N, 2.22.

Observation and Spectroscopic Data for [Pt(1-*H*-P,P)(2'-P,P)Cl] (**7**). In a 5 mm NMR tube, solid **6** (0.030 g, 0.026 mmol) was dissolved in 0.5 mL of CDCl₃, and pure NEt₃ (0.05 mL, 0.36 mmol) was added. The colorless solution turned green immediately, and the formation of **7** was observed spectroscopically. ¹H NMR (CDCl₃, assignments refer to Figure 4): 3.33 (t, 2H, ³J(H,H) = 7.4 Hz, N₂CH₂), 3.43 (t, 2H, ³J(H,H) = 8.6 Hz, N₁CH₂), 3.77 (t, 2H, ³J(H,H) = 8.6 Hz, O₁CH₂), 4.14 (dd, with ¹⁹⁵Pt satellites, 1H, ²J(H,P) = 6.6 Hz, ⁴J(H,P) = 3.5 Hz, ³J(H,Pt) = 40 Hz, H29), 4.42 (t, 2H, ³J(H,H) = 7.4 Hz, O₂CH₂), 6.70–7.54 (m, Ph); ³¹P{¹H} NMR (CDCl₃) (see Figure 4 for labeling): –39.6 (ddd, with Pt satellites, ²J(P₂,P₄) =

8 Hz, ²J(P₂,P₁) = 12 Hz, ²J(P₂,P₃) = 357 Hz, ¹J(P,Pt) = 2074 Hz, P₂), –38.6 (ddd, with Pt satellites, ²J(P₁,P₃) = 9 Hz, ²J(P₁,P₂) = 12 Hz, ²J(P₁,P₄) = 306 Hz, ¹J(P,Pt) = 1934 Hz, P₁), –4.3 (ddd, with Pt satellites, ²J(P₄,P₂) = 8 Hz, ²J(P₄,P₃) = 36 Hz, ²J(P₄,P₁) = 306 Hz, ¹J(P,Pt) = 2208 Hz, P₄), 50.8 (ddd, with Pt satellites, ²J(P₃,P₁) = 9 Hz, ²J(P₃,P₄) = 36 Hz, ²J(P₃,P₂) = 357 Hz, ¹J(P,Pt) = 2539 Hz, P₃).

Observation and Spectroscopic Data for [Pt(1-*H*-P,P)(1-*H*-P,N)] (**8**). Pure NEt₃ (1.00 mL, 7.18 mmol) was added to a stirred solution of ligand **1** (1.15 g, 2.54 mmol) in CH₂Cl₂ (10 mL), and solid [PtCl₂(NPh)₂] (0.300 g, 0.63 mmol) was added. The solution was stirred for 24 h, whereupon a yellow precipitate formed. The volatiles were removed under vacuum conditions, and MeCN (20 mL) was added to the solid. The suspension was filtered (the solid is **3a**), and the filtrate was dried under vacuum conditions. The resulting residue was washed with diethylether (2×30 mL), and the formation of **8** was observed spectroscopically. ¹H NMR (CDCl₃, assignments refer to Figure 5): 3.49 (t, 2H, ³J(H,H) = 8.2 Hz, N₂CH₂), 3.52 (t, 2H, ³J(H,H) = 8.7 Hz, N₁CH₂), 3.75 (t, 2H, ³J(H,H) = 8.7 Hz, O₁CH₂), 4.03 (t, 2H, ³J(H,H) = 8.2 Hz, O₂CH₂), 6.96–7.48 (m, 40H, Ph). ³¹P{¹H} NMR (CDCl₃) (see Figure 5 for labeling): –45.9 (dd, with Pt satellites, ²J(P₁,P₃) = 4 Hz, ²J(P₁,P₂) = 9 Hz, ¹J(P,Pt) = 2462 Hz, P₁), –31.4 (ddd, with Pt satellites, ²J(P₂,P₁) = 9 Hz, ²J(P₂,P₃) = 346 Hz, ⁴J(P₂,P₄) = 17 Hz, ¹J(P,Pt) = 2014 Hz, P₂), –21.0 (dd, with Pt satellites, ⁴J(P₄,P₂) = 17 Hz, ²J(P₄,P₃) = 81 Hz, ³J(P,Pt) = 87 Hz, P₄), 27.3 (ddd, with Pt satellites, ²J(P₃,P₁) = 4 Hz, ²J(P₃,P₂) = 346 Hz, ²J(P₃,P₄) = 81 Hz, ¹J(P,Pt) = 2312 Hz, P₃).

X-Ray Data Collection, Structure Solution, and Refinement for All Compounds. Suitable crystals for the X-ray analysis of all compounds were obtained as described below. The intensity data were collected on a Kappa CCD diffractometer³² (graphite monochromated Mo K α radiation, λ = 0.71073 Å) at 173(2) K for all compounds. Crystallographic and experimental details for the structures are summarized in Table 3. The structures were solved by direct methods (SHELXS-97) and refined by full-matrix least-squares procedures (based on F^2 , SHELXL-97)³³ with anisotropic thermal parameters for all of the non-hydrogen atoms. The hydrogen atoms were introduced into the geometrically calculated positions (SHELXS-97 procedures) and refined riding on the corresponding parent atoms. For $4 \cdot \text{CHCl}_3$, the PLATON ADDSYM algorithm detects an additional (pseudo) translation on *a*, relating the two independent main residues. However, they display a slightly different conformation (rotation of the phenyls around the P–C bond, different mutual orientation of the Au–Cl lines). Consistently, refinement in subcells, e.g., with an halved *a* axis, results in a severely disordered model. In $6 \cdot 2.5\text{CH}_2\text{Cl}_2$, a disorder involved the cocrystallized solvent. Five molecules of dichloromethane were modeled and refined unrestrained. The residual electron density, however, could not be modeled and affected considerably the quality of the main residues. A PLATON SQUEEZE³⁴ procedure was then applied, resulting in improved refinement parameters. In $8 \cdot \text{CH}_2\text{Cl}_2$, a molecule of dichloromethane was found disordered in two positions with equal occupancy factors, sharing a chloride in common. This disordered molecule was refined unrestrained. CCDC 800948 ($3b \cdot 4\text{CH}_2\text{Cl}_2$), 800949 ($4 \cdot \text{CHCl}_3$), 800950 ($6 \cdot 2.5\text{CH}_2\text{Cl}_2$), and 800951 ($8 \cdot \text{CH}_2\text{Cl}_2$) contain the supplementary crystallographic data for this paper and can be obtained free of charge from the Cambridge Crystallographic Data Center via www.ccdc.cam.ac.uk/data_request/cif.

■ ASSOCIATED CONTENT

Supporting Information. NMR spectra and CIF files giving crystallographic data. This material is available free of charge via the Internet at <http://pubs.acs.org>.

■ AUTHOR INFORMATION

Corresponding Author

*Phone: +33 3 68 85 13 08. Fax: +33 3 68 85 13 22. E-mail: braunstein@unistra.fr.

■ ACKNOWLEDGMENT

We thank Lionel Allouche for NMR experiments and Mélanie Boucher for experimental assistance. The work was supported by the CNRS, the Ministère de l'Enseignement Supérieur et de la Recherche, and the Agence Nationale de la Recherche (ANR-06-BLAN 410).

DEDICATION

†Dedicated to Prof. Wolfgang Kaim on the occasion of his 60th birthday, with our congratulations and best wishes

■ REFERENCES

- (1) (a) Mague, J. T. *J. Cluster Sci.* **1995**, *6*, 217–269. (b) Puddephatt, R. J. *Chem. Soc. Rev.* **1983**, *12*, 99–127.
- (2) (a) Lang, H.-F.; Fanwick, P. E.; Walton, R. A. *Inorg. Chim. Acta* **2002**, *328*, 232–236. (b) Mague, J. T.; Hawbaker, S. W. *J. Chem. Crystallogr.* **1997**, *27*, 603–608. (c) McNair, R. J.; Pignolet, L. H. *Inorg. Chem.* **1986**, *25*, 4717–4723. (d) McNair, R. J.; Nilsson, P. V.; Pignolet, L. H. *Inorg. Chem.* **1985**, *24*, 1935–1939. (e) Anderson, M. P.; Tso, C. C.; Mattson, B. M.; Pignolet, L. H. *Inorg. Chem.* **1983**, *22*, 3267–3275. (f) Anderson, M. P.; Pignolet, L. H. *Organometallics* **1983**, *2*, 1246–1247.
- (3) Mague, J. T.; Krinsky, J. L. *Inorg. Chem.* **2001**, *40*, 1962–1971.
- (4) Mague, J. T.; Johnson, M. P. *Organometallics* **1990**, *9*, 1254–1269.
- (5) Mattson, B. M.; Ito, L. N. *Organometallics* **1989**, *8*, 391–395.
- (6) Anderson, M. P.; Mattson, B. M.; Pignolet, L. H. *Inorg. Chem.* **1983**, *22*, 2644–2647.
- (7) Abdul, J. M.; Fujinami, S.; Honjo, T.; Nishikawa, H. *Polyhedron* **2001**, *20*, 1071–1078.
- (8) See, e.g.: (a) Mantilli, L.; Gérard, D.; Torche, S.; Besnard, C.; Mazet, C. *Chem.—Eur. J.* **2010**, *16*, 12736–12745. (b) Chavez, P.; Rios, I. G.; Kermagoret, A.; Pattacini, R.; Meli, A.; Bianchini, C.; Giambastiani, G.; Braunstein, P. *Organometallics* **2009**, *28*, 1776–1784. (c) Schrems, M. G.; Neumann, E.; Pfaltz, A. *Angew. Chem., Int. Ed.* **2007**, *46*, 8274–8276. (d) Speiser, F.; Braunstein, P.; Saussine, L. *Organometallics* **2004**, *23*, 2633–2640. (e) Speiser, F.; Braunstein, P.; Saussine, L.; Welter, R. *Organometallics* **2004**, *23*, 2613–2624. (f) Braunstein, P.; Naud, F.; Graiff, C.; Tiripicchio, A. *Chem. Commun.* **2000**, 897–898. (g) Lloyd-Jones, G. C.; Pfaltz, A. *Z. Naturforsch., B: Chem. Sci.* **1995**, *50*, 361–367. (h) Sprinz, J.; Helmchen, G. *Tetrahedron Lett.* **1993**, *34*, 1769–1772.
- (9) Pattacini, R.; Margraf, G.; Messaoudi, A.; Oberbeckmann-Winter, N.; Braunstein, P. *Inorg. Chem.* **2008**, *47*, 9886–9897.
- (10) For a recent example, see: Kornev, A. N.; Belina, N. V.; Sushev, V. V.; Panova, J. S.; Lukyanova, O. V.; Ketkov, S. Y.; Fukin, G. K.; Lopatin, M. A.; Abakumov, G. A. *Inorg. Chem.* **2010**, *49*, 9677–9682.
- (11) O'Reilly, M.; Pattacini, R.; Braunstein, P. *Dalton Trans.* **2009**, 6092–6095.
- (12) For a recent example, see: Belina, N. V.; Kornev, A. N.; Sushev, V. V.; Fukin, G. K.; Baranov, E. V.; Abakumov, G. A. *J. Organomet. Chem.* **2010**, *695*, 637–641.
- (13) Fei, Z.; Biricik, N.; Zhao, D.; Scopelliti, R.; Dyson, P. J. *Inorg. Chem.* **2004**, *43*, 2228–2230.
- (14) (a) Baiget, L.; Batsanov, A. S.; Dyer, P. W.; Fox, M. A.; Hanton, M. J.; Howard, J. A. K.; Lane, P. K.; Solomon, S. A. *Dalton Trans.* **2008**, 1043–1054. (b) Margraf, G.; Pattacini, R.; Messaoudi, A.; Braunstein, P. *Chem. Commun.* **2006**, 3098–3100.
- (15) Zhang, S.; Pattacini, R.; Braunstein, P. *Organometallics* **2010**, *29*, 6660–6667.
- (16) (a) Fernandez, E. J.; Gimeno, M. C.; Jones, P. G.; Laguna, A.; Olmos, E. *Organometallics* **1997**, *16*, 1130–1136. (b) Phillips, I. G.; Ball, R. G.; Cavell, R. G. *Inorg. Chem.* **1988**, *27*, 4038–4045.
- (17) Cotton, F. A.; Diebold, M. P.; Matusz, M. *Polyhedron* **1987**, *6*, 1131–1134.
- (18) Ortega, J. V.; Khin, K.; van der Veer, W. E.; Ziller, J.; Hong, B. *Inorg. Chem.* **2000**, *39*, 6038–6050.
- (19) Ruiz, J.; Mosquera, M. E. G.; Garcia, G.; Marquinez, F.; Riera, V. *Angew. Chem., Int. Ed.* **2005**, *44*, 102–105.
- (20) Pickaert, G.; Douce, L.; Ziessel, R.; Cesario, M. *Chem. Commun.* **2000**, 1125–1126.
- (21) Ruiz, J.; Quesada, R.; Riera, V.; Castellano, E.; Piro, O. *Organometallics* **2004**, *23*, 175–177.
- (22) Hamada, A.; Braunstein, P. *Inorg. Chem.* **2009**, *48*, 1624–1637.
- (23) (a) Braunstein, P.; Jud, J.-M.; Dusaosoy, Y.; Fischer, J. *Organometallics* **1983**, *2*, 180–183. (b) Braunstein, P.; Guarino, N.; de Méric de Bellefon, C.; Richert, J.-L. *Angew. Chem., Int. Ed. Engl.* **1987**, *26*, 88–89.
- (24) Goodfellow, R. J.; Taylor, B. F. *J. Chem. Soc., Dalton Trans.* **1974**, 1676–1684.
- (25) Park, Y. J.; Sickerman, N. S.; Ziller, J. W.; Borovik, A. S. *Chem. Commun.* **2010**, 46, 2584–2586.
- (26) Pattacini, R.; Giansante, C.; Ceroni, P.; Maestri, M.; Braunstein, P. *Chem.—Eur. J.* **2007**, *13*, 10117–10128.
- (27) Braunstein, P.; Naud, F.; Rettig, S. J. *New J. Chem.* **2001**, *25*, 32–39.
- (28) For example, see: Lai, S.-W.; Chan, M. C.-W.; Cheung, T.-C.; Peng, S.-M.; Che, C.-M. *Inorg. Chem.* **1999**, *38*, 4046–4055.
- (29) (a) Hartley, F. R. *The Chemistry of Platinum and Palladium*; Applied Science Publishers: London, 1973. (b) Braunstein, P.; Bender, R.; Jud, J. *Inorg. Synth.* **1989**, *26*, 341–350.
- (30) Uson, R.; Laguna, A.; Laguna, M. *Inorg. Synth.* **1989**, *26*, 85–91.
- (31) For a comparable $^1J(\text{C},\text{P})$ coupling value in $[\text{Pd}(\text{dmba})(\text{PCH-oxazoline})]$ (dmba = *N,N*-dimethyl-benzylamine), see ref 27.
- (32) *Kappa CCD Reference Manual*; Bruker-Nonius BV: The Netherlands, 1998.
- (33) Sheldrick, G. M. *Acta Crystallogr.* **2008**, *A64*, 112–122.
- (34) van der Sluis, P.; Spek, A. L. *Acta Crystallogr., Sect. A* **1990**, *46*, 194–201.

■ NOTE ADDED AFTER ASAP PUBLICATION

This paper was published on the Web on March 15, 2011, with a minor error in the Abstract. The corrected version was reposted on March 18, 2011.